Resolvin D1 Improves the Resolution of Inflammation via Activating NF-κB p50/p50–Mediated Cyclooxygenase-2 Expression in Acute Respiratory Distress Syndrome

Ye Gao,*,[1] Huawei Zhang,*,[1] Lingchun Luo,* Jing Lin,* Dan Li,* Sisi Zheng,* Hua Huang,* Songfan Yan,* Jingxiang Yang,* Yu Hao,* Hui Li,* Fang Gao Smith,*,[†] and Shengwei Jin*

Acute respiratory distress syndrome (ARDS) is a severe illness characterized by uncontrolled inflammation. The resolution of inflammation is a tightly regulated event controlled by endogenous mediators, such as resolvin D1 (RvD1). Cyclooxygenase-2 (COX-2) has been reported to promote inflammation, along with PGE_2, in the initiation of inflammation, as well as in prompting resolution, with PGD_2 acting in the later phase of inflammation. Our previous work demonstrated that RvD1 enhanced COX-2 and PGD_2 expression to resolve inflammation. In this study, we investigated mechanisms underlying the effect of RvD1 in modulating proresolving COX-2 expression. In a self-limited ARDS model, an LPS challenge induced the biphasic activation of COX-2, and RvD1 promoted COX-2 expression during the resolution phase. However, it was significantly blocked by treatment of a NF-κB inhibitor. In pulmonary fibroblasts, NF-κB p50/p50 was shown to be responsible for the proresolving activity of COX-2. Additionally, RvD1 potently promoted p50 homodimer nuclear translocation and robustly triggered DNA-binding activity, upregulating COX-2 expression via lipoxin A_4 receptor/formyl peptide receptor 2. Finally, the absence of p50 in knockout mice prevented RvD1 from promoting COX-2 and PGD_2 expression and resulted in excessive pulmonary inflammation. In conclusion, RvD1 expedites the resolution of inflammation through activation of lipoxin A_4 receptor/formyl peptide receptor 2 receptor and NF-κB p50/p50–COX-2 signaling pathways, indicating that RvD1 might have therapeutic potential in the management of ARDS. ***The Journal of Immunology*****, 2017, 199: 2043–2054.**

Acute respiratory distress syndrome (ARDS) is a common and potentially fatal critical condition that is associated with high mortality (1). Despite decades of efforts to improve the prognosis of ARDS, no pharmacological interventions have been proven to be effective. Thus ARDS is a considerable worldwide health burden (2, 3). The main pathophysiologic mechanism underlying ARDS is unrestrained and perpetual inflammation, resulting in extensive alveolar barrier disruption and abundant extravascular accumulation of protein-rich edema fluid. The respiratory failure leads to multiorgan dysfunction and then death (4). Therefore, the timely resolution of inflammation is thought to be pivotal in restoring homeostasis. The resolution of inflammation is a highly ordered and active process driven by novel mediators and endogenously controlled mechanisms (5). Therefore, identification of proresolving agonists or biochemical compounds could offer novel insight into the treatment of ARDS (6).

Cyclooxygenase-2 (COX-2), an inducible enzyme, catalyzes the conversion of diverse PGs. In addition to its well-known role as a pharmaceutical target for anti-inflammatory drugs in inflammatory diseases, COX-2 also exerts versatile biological activities to resolve inflammation (7–9). At the onset of inflammation, COX-2 has a potent proinflammatory effect, predominantly through the generation of PGE_2, whereas in the resolution phase, COX-2 is responsible for producing proresolving PGs, such as PGD_2, 15-deoxy-$\Delta^{12,14}$-PGJ_2, and $PGF_{2\alpha}$ (10–13). Notably, PGE_2 and PGD_2 are responsible for modulating lipid mediator class switching from proinflammation to proresolution, as they have been shown to initiate the production of 15-lipoxygenase, a pivotal enzyme that is capable of mediating the biosynthesis of proresolving lipid mediators (14). In ARDS, COX-2 displayed pivotal actions in facilitating resolution through its ability to generate proresolving lipid mediators, such as lipoxin A_4 (15), and both the genetic disruption and pharmacological blocking of COX-2 expression have been shown to lead to robust inflammation and aggressive lung injury (10–12). Furthermore, COX-2 is also responsible for hepatocyte growth factor secretion, which contributes to the restoration of healthy alveolar epithelium (16). Several signaling pathways are involved in regulating of COX-2 expression, including the ERK, AKT, PI3K, and NF-κB pathways. However, the pathway that mediates proresolving COX-2 activation has not been fully clarified.

*Department of Anesthesia and Critical Care, The Second Affiliated Hospital and Yuying Children's Hospital of Wenzhou Medical University, Zhejiang 325027, China; and [†]Institute of Inflammation and Ageing, College of Medical and Dental Science, University of Birmingham, Birmingham B15 2WB, United Kingdom

[1]Y.G. and H.Z. contributed equally to this work.

ORCIDs: 0000-0001-6882-6886 (Y.G.); 0000-0003-0034-9213 (H.Z.); 0000-0002-1866-0010 (H.H.); 0000-0002-8351-1206 (Y.H.); 0000-0002-8095-0609 (F.G.S.).

Received for publication February 28, 2017. Accepted for publication June 30, 2017.

This work was supported by National Natural Science Foundation of China Grants 81570076 and 81571862.

Address correspondence and reprint requests to Dr. Shengwei Jin or Dr. Fang Gao Smith, Department of Anesthesia and Critical Care, The Second Affiliated Hospital and Yuying Children's Hospital of Wenzhou Medical University, 109 Xueyuan Road, Wenzhou, Zhejiang 325027, China (S.J.) or Institute of Inflammation and Ageing, College of Medical and Dental Science, University of Birmingham, Birmingham B15 2WB, U.K. (F.G.S.). E-mail addresses: jinshengwei69@163.com (S.J.) or f.g.smith@bham.ac.uk (F.G.S.)

Abbreviations used in this article: ALX/FPR2, lipoxin A_4 receptor/formyl peptide receptor 2; ARDS, acute respiratory distress syndrome; COX-2, cyclooxygenase-2; GPR32, G protein–coupled receptor 32; KO, knockout; MPO, myeloperoxidase; RvD1, resolvin D1; SD, Sprague Dawley; WT, wild-type.

Pulmonary fibroblasts are mesenchymal cells with well-recognized roles in lung remodeling and repair. They also act as innate immune sentinels that modify inflammation and orchestrate its resolution (17). While activated, fibroblasts secrete various inflammatory mediators that amplify the immune response (18). Additionally, fibroblasts have emerged as regulators of inflammation resolution that act by producing proresolving peroxisome proliferator–activated receptor-γ ligands (19), as well as COX-2 and PGD_2 (20). Recently, accumulating evidence has demonstrated that the growth factors secreted from fibroblasts can promote alveolar barrier function (21–23), alleviate pulmonary edema (21, 24), and protect against lung injury from various stresses, such as LPS (25, 26), ventilator (24) and ischemia/reperfusion–induced lung injury (27, 28). Thus, lung fibroblasts have emerged as essential players in the resolution of ARDS.

Resolvin D1 (RvD1; 7*S*,8*R*,17*S*-trihydroxy-4*Z*,9*E*,11*E*,13*Z*,15*E*,19*Z*-docosahexaenoic acid), an endogenous specialized proresolving lipid mediator, is derived from omega-3 docosahexaenoic acid during the resolution phase of acute inflammation and displays potent anti-inflammatory and proresolving activities (29, 30). RvD1 has consistently been shown to impede inappropriate neutrophil infiltration, suppress excessive inflammatory mediator production, accelerate efferocytosis (18), and promote the clearance of alveolar fluid (31) to perform its protective roles in ARDS. Moreover, RvD1 markedly reduces acute lung injury–associated mortality through curbing NF-κB activation and COX-2 expression (32). Notably, our previous study illustrated that RvD1 exerted an anti-inflammatory effect by altering COX-2 expression in the proinflammatory phase, whereas it also collaborated with the proresolving COX-2 activation in fibroblasts during the resolution phase (20), convincingly demonstrating its potent role in maintaining homeostasis.

However, no studies to date have addressed whether RvD1 potentiates inflammation resolution by modulating proresolving COX-2 expression in vivo or identified the underlying mechanism involved in RvD1-mediated COX-2 regulation. In this study, we present evidence for a self-limited experimental model of ARDS in which RvD1 facilitates inflammation resolution via upregulating proresolving COX-2 activity, in part by promoting the activation of NF-κB p50/p50, which protects the lung from LPS-initiated injury.

Materials and Methods

Materials

RvD1 was purchased from Cayman Chemical (Ann Arbor, MI). LPS (*Escherichia coli* O55: B5), SP600125 (a JNK inhibitor), and SB203580 (a p38 MAPK inhibitor) were obtained from Sigma-Aldrich (St. Louis, MO). MG-132 (an NF-κB inhibitor) was purchased from Tocris Bioscience (Bristol, U.K.). BOC-2 (a lipoxin A_4 receptor/formyl peptide receptor 2 [ALX/FPR2] inhibitor) was obtained from Biomol/Enzo Life Sciences (Farmingdale, NY). DMEM and FBS were purchased from Life Technologies BRL (Grand Island, NY). A nuclear protein extraction kit was obtained from Thermo Scientific (Rockford, IL). Primary Abs against COX-2, p105/p50, p65, RelB, and lamin B1 were purchased from Abcam (Cambridge, U.K.). PGE_2, PGD_2, myeloperoxidase (MPO), and TNF-α ELISA kits were purchased from R&D Systems (Minneapolis, MN). Protein levels were determined using a bicinchoninic acid kit (Thermo Scientific).

Animal preparation

Male Sprague Dawley (SD) rats (250–300 g; SLAC Laboratory, Shaghai, China), wild-type (WT) C57BL/6 mice (6–12 wk, SLAC Laboratory), and NF-κB p50 knockout (KO) mice (6–12 wk, B6;129P2-*Nfkb1*^{tm1Bal}/J; The Jackson Laboratory) were maintained under specific pathogen-free conditions in a full-barrier facility until experiments were performed.

An LPS-induced ARDS model was generated via i.v. injections of LPS into tail veins as previously described (31). The animal experiments were performed using the methods described below.

SD rats and WT C57BL/6 mice were treated with 3 mg/kg body weight of LPS administered via i.v. injections, and control animals were administered the same volume of sterile 0.9% saline i.v. to characterize lung injury over time. Animals were euthanized at the following time points: 6, 12, 24, 48, and 72 h after i.v. injection.

For the experiment involving MG-132 and RvD1 treatments in rats, MG-132 was dissolved in DMSO and then diluted in 500 μl of sterile 0.9% saline for injection. Twelve hours after the i.v. LPS (3 mg/kg) injection or a sham injection of saline, rats were given RvD1 (5 μg/kg) or an equivalent volume of ethanol via tail vein injection. For treatment, rats were administered MG-132 i.v.1 h prior to RvD1 injection, whereas other groups received an equal volume of DMSO/saline solution. Rats were sacrificed 24 h after LPS exposure.

For the comparison between WT and p50 KO mice, RvD1 (5 μg/kg) injections or sham injections of saline were administered 24 h after an i.v. injection of LPS (3 mg/kg). All mice were humanely killed 48 h after LPS exposure while under anesthesia.

Histological analysis of lung tissues

For histological examinations, the right lung of each animal was fixed in 10% paraformaldehyde for 24 h, embedded in paraffin wax, sectioned, and stained with H&E for light microscopy analysis. Lung injury scores were quantified by an investigator who was blinded to the treatment groups using an established histopathological scoring system (31).

Cell culture

Rat pulmonary fibroblasts were isolated from 2- to 3-d-old SD rats, and murine pulmonary fibroblasts were isolated from C57BL/6 mice, as previously described (20). Cells were used at early passages (P3–P5).

For all experiments, cells (5×10^5) were plated in six-well plates and grown to 80% confluence. Fibroblasts were allowed to remain in a quiescent state for 24 h by incubating them in medium containing 0.5% FBS prior to treatment. After 24 h of culture with LPS (1 μg/ml) or a control medium, fibroblasts were treated with 100 nM RvD1 or a vehicle solution (0.1% ethanol, as the RvD1 was supplied in ethanol) for an additional 24 h. SP600125 (10 μM), SB603580 (10 μM), MG-132 (10 μM), and BOC-2 (10 μM) were added 30 min prior to RvD1 administration.

Measurement of TNF-α, MPO, PGE_2, and PGD_2 production

TNF-α, MPO, PGE_2, and PGD_2 concentrations were measured in homogenized lung tissues, and culture supernatants were collected as previously described (20, 33) using ELISA kits (R&D Systems) according to the manufacturer's instructions. Assays were run in triplicate and repeated twice.

Protein extraction and Western blot analysis

Nuclear proteins were extracted using a nuclear extract kit (Thermo Scientific) according to the manufacturer's instruction. Whole protein samples were prepared by suspending cells or tissues directly in RIPA lysis buffer (50 mM Tris [pH 7.4], 150 mM NaCl, 1% Triton X-100, 1% sodium deoxycholate, 0.1% SDS, 1 mg/ml leupeptin sodium orthovanadate, sodium fluoride, and EDTA) and 1 mM PMSF for 1 h on ice. This was followed by centrifugation for 30 min at 12,000 × *g*.

Protein lysates were electrophoresed via 10% SDS-PAGE, and the separated proteins were transferred to a polyvinyl difluoride membrane. After the membranes were blocked in 5% dry skim milk/TBST buffer (TBS containing 0.1% Tween-20) for 1 h at room temperature, they were incubated with primary Abs for COX-2, p65, p50, RelB, lamin B1, and β-actin overnight at 4°C. This was followed by treatment with the appropriate secondary Abs for 1 h. The proteins were detected using chemiluminescence reagents (Thermo Scientific). Images were scanned with a UVP imaging system and analyzed using an ImageQuant LAS 4000 mini system (GE Healthcare Bio-Sciences AB, Uppsala, Sweden).

EMSA and supershift assay

Nuclear extracts were prepared from lung tissues and fibroblasts treated as described above. The EMSA was performed using a nonradioactive NF-κB EMSA kit according to the manufacturer's instructions (Thermo Scientific). The sequence of the NF-κB probe was 5′-AGTTGAGGGGACTTTCCCAGGC-3′ and that of the mutant probe was 5′-AGTTGAGGCTACTTTCCCAGGC-3′. Biotins were labeled with 5′ end oligonucleotides. Then, 15 μg of crude nuclear protein were incubated with a 15 μl binding reaction system including 1.5 μl of 10× binding buffer, 1.5 μl of poly(dI:dC) (1.0 μg/μl), and ddH_2O to a final volume of 10 μl for 20 min at room temperature. Bio-NF-κB or Bio-mutant-NF-κB probes were then added, and the reaction mixture was incubated for 20 min at room temperature. Where indicated, 1 and 2 μl of

specific cold competitor oligonucleotide were added in a 100× competing system before the labeled probe was added, and samples were then incubated for 20 min. Protein–DNA complexes were resolved via electrophoresis at 4°C on a 6.5% acrylamide gel and subjected to autoradiography. Electrophoresis was performed on a 6.5% nondenaturing polyacrylamide gel at 175 V in 0.25× TBE (1× TBE consists of 89 mM Tris-HCl, 89 mM boric acid, and 5 mM EDTA [pH 8]) at 4°C for 1 h. Gels were transferred to banding membranes at 394 mA in 0.5× TBE (1× TBE consists of 89 mM Tris-HCl, 89 mM boric acid, and 5 mM EDTA [pH 8]) at room temperature for 40 min. Then, the membranes were crosslinked in a UV crosslink apparatus for 10 min (immobilization), blocked, labeled with streptavidin-HRP, washed, and equilibrated. Membrane images were acquired with an Imager apparatus (Alpha Innotech). For the Ab supershift assay, 5 μg of Ab specific to NF-κB p50, p65, or RelB was incubated on ice with the nuclear protein extract for 30 min prior to the addition of the reaction mixture containing radiolabeled nucleotides.

Statistical analysis

Data are presented as mean ± SEM. All data were analyzed using a Student *t* test or one-way ANOVA, followed by a Tukey test for post hoc comparisons. A p value <0.05 was considered significant. Statistical analyses were performed using Prism 6.0 software (GraphPad Software, San Diego, CA).

Results

Characterization of the rat LPS-induced ARDS model

To assess pathological changes in the lung, H&E staining was used in our study as shown in Fig. 1A. In contrast to the normal lung parenchyma in the control group, the lung architecture in the experimental group showed distinct changes over time after LPS administration. This was accompanied by significant inflammatory cells infiltration, interstitial edema, extensive thickening of the alveolar septum, demolished structure of the pulmonary alveoli, and hemorrhaging, and these effects were evident at 6 h after LPS administration, subsequently peaked at 12 h, and then were gradually ameliorated. Acute lung injury scores were quantified in parallel with the pathophysiological changes (Fig. 1B). Additionally, the proinflammatory cytokine TNF-α rapidly increased at 12 h and then declined gradually (Fig. 1C). Lung MPO expression, reflecting neutrophil activity, also peaked at 12 h and subsequently decreased (Fig. 1D). These data suggest that a resolution period starts within ∼12 h after LPS exposure.

Time dependence of pulmonary COX-2 activation in a rat model of LPS-induced ARDS

Having characterized the inflammation induction and resolution phases of the ARDS model in terms of histological changes and chemokine productions, we next assessed the dynamic changes in COX-2 expression induced by LPS using Western blot analysis. COX-2 showed a biphasic expression pattern during the course of the experiment (Fig. 2A). The COX-2 expression initially peaked at the onset of inflammation 6 h after LPS exposure, and a second peak was detected during the resolution stage 24 h after exposure. Moreover, the first peak in COX-2 expression was coincident with the maximum PGE_2 expression (Fig. 2B), and the highest level of PGD_2 production was associated with the second COX-2 peak (Fig. 2C). Taken together, these confirmed findings indicated that COX-2 is proinflammatory during the early stage of inflammation but plays a role in inflammation resolution at the later stage.

RvD1 facilitates the resolution of inflammation by promoting NF-κB p50-derived COX-2 expression in the ARDS model

In the LPS-induced ARDS model, the administration of RvD1 in the resolution phase effectively promoted the repair of damaged pulmonary histology, as indicated by H&E staining (Fig. 3A), resulting in the nearly complete restoration of the morphological and histological changes in pulmonary tissue caused by LPS exposure to a state that was comparable to the condition of the control group (Fig. 3A). However, administering the NF-κB inhibitor MG-132 to rats reversed the proresolving effects of RvD1 and substantially aggravated the damage in the LPS group, resulting in pronounced interstitial edema, hemorrhaging, thickening of alveolar walls, and inflammatory cell infiltrations (Fig. 3A). Consistent with the pathophysiological changes, there was a significant difference between the LPS plus RvD1 group and LPS plus RvD1 plus MG-132 group ($p < 0.01$) and between the LPS and LPS plus MG-132 groups ($p < 0.01$) (Fig. 3B).

Furthermore, RvD1 was found to dramatically increase COX-2 protein expression during the resolution phase (Fig. 3C). To assess the mechanism underlying the effect of the RvD1 on COX-2 in the later phase of inflammation, we injected MG-132 at 1 h prior to RvD1 administration, and this significantly decreased COX-2 expression (Fig. 3C). Similarly, the NF-κB activation triggered by RvD1 was clearly suppressed by MG-132 (Fig. 3D). Moreover, the supershift assay results showed that only p50 subunits, and not p65 subunits, were detected in the LPS plus RvD1 group (Fig. 3D), indicating that NF-κB p50/p50 was responsible for the RvD1-induced increase in COX-2 expression during the resolution phase.

NF-κB is responsible for proresolving COX-2 protein expression in pulmonary fibroblasts

Considering the pivotal role of fibroblasts in ARDS resolution, pulmonary fibroblasts were used to verify the protective roles of RvD1 in vitro. As our previous study confirmed that the secondary peak in COX-2 expression in newborn rat pulmonary fibroblasts occurred at 48 h after LPS stimulation (20), 48 h was chosen as the time point in the resolution phase that was analyzed in this experiment.

Intracellular COX-2 regulatory signaling pathways are remarkably complex and included the activation of the JNK, p38 MAPK, and NF-κB signaling pathways (34). We assessed the mechanism underlying COX-2 expression in the resolution phase by administering specific JNK, p38 MAPK, and NF-κB inhibitors to verify their association with COX-2 expression. As expected, COX-2 expression in primary pulmonary fibroblasts was dramatically increased by exposure to LPS for 48 h, and there were no significant changes between the control, SP600125, SB203580, and MG-132 groups (Fig. 4). Notably, only MG-132 significantly suppressed LPS-induced COX-2 production ($p < 0.01$), whereas inhibitors of JNK (SP600125) and p38 MAPK(SB203580) had no significant effect on COX-2 expression (Fig. 4).

NF-κB p50/p50 formation is activated in the resolution phase in LPS-stimulated pulmonary fibroblasts

The time course of LPS-induced NF-κB activation was examined using EMSA to explore whether NF-κB exhibits biphasic peaks similar to those exhibited by COX-2 during the initiation and resolution of inflammation. Although no prominent biphasic activation of NF-κB was observed during the progression of inflammation, NF-κB was activated by LPS in the resolution phase (Fig. 5A).

Because the NF-κB family consists of structurally homologous transcription factors, including p65, p105/p50, p100/p52, RelB, and c-Rel, which form various homo- or heterodimers to regulate diverse biological processes (35), we further examined which dimers were responsible for inducing COX-2 expression associated with the resolution of inflammation. Western blot analyses of nuclear protein extracts were performed to verify nuclear translocation of NF-κB. Analyses showed that only the nuclear levels of the NF-κB p50 subunit protein expression were significantly in the LPS group compared with the control group ($p < 0.01$) (Fig. 5B).

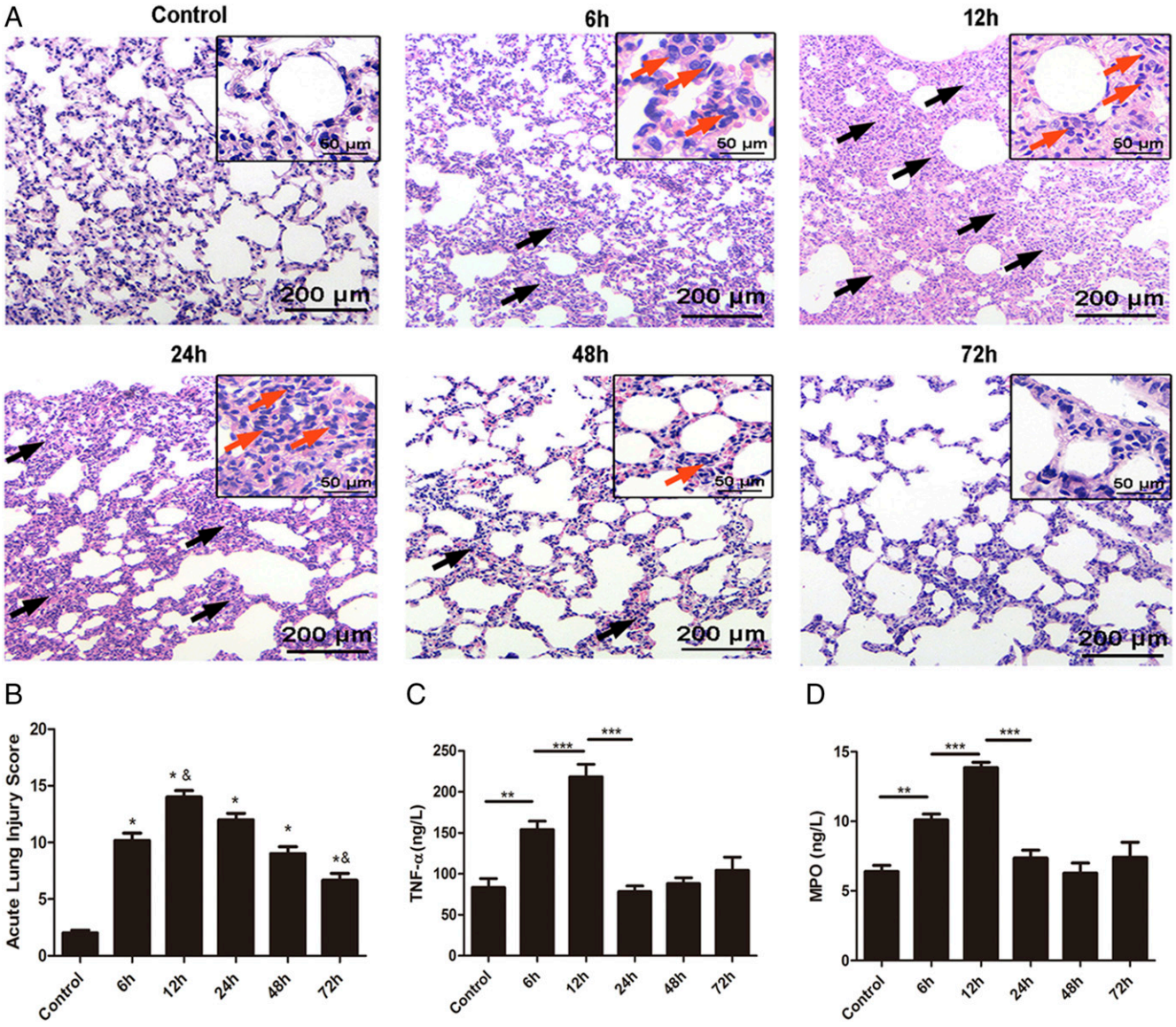

FIGURE 1. Characterization of the rat LPS-induced ARDS model. LPS (3 mg/kg) or an equivalent volume of sterile 0.9% saline was i.v. administered to SD rats, which were stimulated at the indicated time points. (**A**) Representative photomicrographs of pulmonary histology shown by H&E staining, Original magnification, ×100 (inset, ×400). LPS-induced lung inflammation is characterized by marked edema, thickened alveolar walls (black arrows), and an alveolar infiltrate rich in neutrophils (red arrows). (**B**) Acute lung injury score. (**C** and **D**) The concentrations of TNF-α and MPO in homogenized lung tissue were measured via ELISA. Data are shown as mean ± SEM, n = 6–8 rats per treatment, and are representative of three independent experiments. $^{*}p < 0.05$ compared with the control group, $^{\&}p < 0.05$ compared with the 6 h group, $^{**}p < 0.01$, $^{***}p < 0.001$.

Given that NF-κB is an inducible transcription factor and is activated in the resolution phase, supershift experiments were performed on fibroblasts to identify the activated forms of NF-κB using anti-p65, anti-p50, and anti-RelB Abs. Only the p50 subunit was detectable, as evident by the presence of a complex with a shifted band that migrated at a higher molecular mass (Fig. 5C). Thus, only p50 exerts its DNA-binding activity following translocation into the nucleus. Because the p50 subunit forms a homo- or heterodimer complex of p65/p50 or p50/p50, these findings suggest that p50/p50 homodimers preferentially form in the resolution phase of LPS-induced inflammation, as few shifted bands containing p65 were detected in the supershift assays.

RvD1-mediated promotion of COX-2 expression in fibroblasts is regulated by ALX/FPR2–NF-κB p50/p50 activation

Because LPS-induced COX-2 expression primarily depends on the activation of NF-κB p50/p50 and the RvD1-induced inhibition of proinflammatory COX-2 expression is mediated by ALX/FPR2 in a murine model of ARDS (32), we assessed whether RvD1 could modulate proresolving COX-2 expression via the ALX/FPR2–NF-κB p50/p50 signaling pathway. As shown in Fig. 6A, the nuclear translocation of NF-κB p50/p50 in the resolution stage was markedly promoted by cotreatment with RvD1. Consistent with the results of the Western blot analysis, RvD1 also increased the DNA-binding activity of NF-κB in LPS-stimulated fibroblasts (Fig. 6B), indicating that RvD1 had a positive effect on NF-κB p50/p50 activation.

To confirm whether LPS-induced COX-2 production in inflammatory resolution is regulated by RvD1 via NF-κB p50/p50 activation, we isolated primary pulmonary fibroblasts from WT and p50 KO mice to compare the effects of RvD1 on COX-2 expression. In the absence of LPS stimulation, COX-2 expression was not observed in either WT or p50 KO mice (Fig. 6C), whereas it was dramatically reduced in the p50 KO mice following

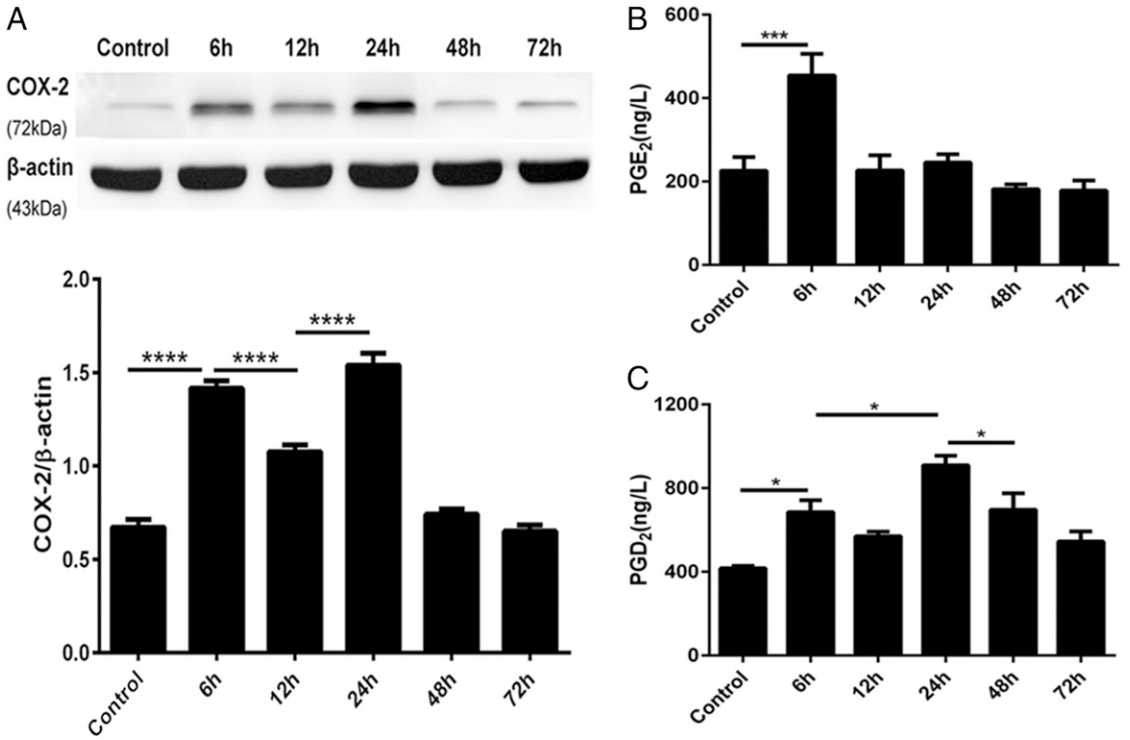

FIGURE 2. Time dependence of pulmonary COX-2 activation in a rat model of LPS-induced ARDS. LPS (3 mg/kg) or an equivalent volume of sterile 0.9% saline was i.v. administered to SD rats, which were stimulated for the indicated durations. Lung tissue samples were collected after LPS administration for Western blot and ELISA analysis. (**A**) COX-2 protein expression was assessed via Western blot and analyzed via densitometry. Values were compared with β-actin expression. (**B** and **C**) PGE_2 and PGD_2 concentrations in homogenized lung tissue were measured via ELISA. Data are shown as mean ± SEM, $n = 6$–8 rats per time point per group, and are representative of four independent experiments. $^*p < 0.05$, $^{***}p < 0.001$, $^{****}p < 0.0001$.

RvD1 and LPS cotreatment. In contrast to the augmentation of COX-2 expression caused by RvD1 in WT pulmonary fibroblasts, the promotional effect of RvD1 on COX-2 expression was blocked in p50-deficient fibroblasts (Fig. 6C). Additionally, BOC-2 (10 μM), an ALX/FPR2 antagonist, was used to measure changes in COX-2 expression in LPS-stimulated pulmonary fibroblasts by Western blot. As shown in Fig. 6D, BOC-2 abrogated the effect of RvD1 on COX-2 expression. Thus, RvD1 may increase COX-2 expression during the resolution of inflammation by regulating NF-κB p50/p50 activation, which depends on the ALX/FPR2 receptor.

p50-deficient mice display impaired inflammation resolution and diminished COX-2 expression following RvD1 treatment

Given that NF-κB p50/p50 is responsible for the stimulatory effect of RvD1 on COX-2 expression in the resolution phase, we prepared p50-deficient mice to further identify the mechanism underlying the effect of RvD1 in vivo. In this study, we also modeled ARDS with an i.v. LPS injection, as previously described.

As shown in Fig. 7A, LPS injections in C57BL/6 mice resulted in early COX-2 expression, which peaked at 6 h and was comparable to the expression pattern observed in SD rats, whereas the second COX-2 activation peak in mice occurred at 48 h and was less prominent than the peak observed at 6 h. Therefore, mice displayed a biphasic COX-2 activation pattern, similar to the rat ARDS model.

Using p50 KO mice and their WT littermates, we investigated whether NF-κB p50 plays an essential role in the regulatory effects of RvD1 on COX-2 expression during the later stage of inflammation. In WT mice, RvD1 administration significantly reversed the pathological changes induced by LPS, whereas there was no significant variation in the histological results between the LPS plus RvD1 and LPS groups in p50 KO mice, which all showed apparent interstitial edema, neutrophil infiltration, hemorrhaging, alveolar disarray, and thickness of the alveolar septum (Fig. 7B). Of note, the increased COX-2 expression induced by RvD1 in WT mice was considerably diminished in p50 KO mice (Fig. 7C). As for PG productions, strikingly, the expression of both PGE_2 and PGD_2 was significantly increased in the lungs of p50 KO mice following LPS injection, and both PGs tended to be present at lower levels than in the control group. There was no positive feedback on PGE_2 induced by RvD1 in WT or p50 KO mice. However, PGE_2 concentrations were significantly lower in p50 KO mice ($p < 0.05$) (Fig. 7D). Additionally, PGD_2 production was significantly promoted by RvD1 and LPS cotreatment in WT mice. The p50 deficiency suppressed LPS-induced PGD_2 and also impaired the stimulatory effect of RvD1 (Fig. 7E). Collectively, these data indicate that NF-κB p50 accounts for the RvD1-mediated promotion of COX-2 involved in facilitating inflammation resolution.

Discussion

In the present study, we confirmed the novel proresolution capacities of RvD1 in ARDS. Our data showed that there was a biphasic COX-2 activation pattern in the ARDS model and that NF-κB p50/p50 homodimers were responsible for altering COX-2 expression in the resolution stage of inflammation. RvD1 administration markedly increased COX-2 expression, as well as subsequently increasing proresolving PGD_2 production, resulting in potently prompting inflammation resolution (summarized in Fig. 8). However, the inhibition or deletion of p50 eliminated the stimulatory effect of RvD1 on COX-2 production and removed the acceleration of resolution.

The resolution of an acute inflammation is an active process that is crucial for restoring homeostasis. In most cases, acute lung injury, the mild form of ARDS, spontaneously resolves, indicating the existence of internal, host-protective signaling pathways in the

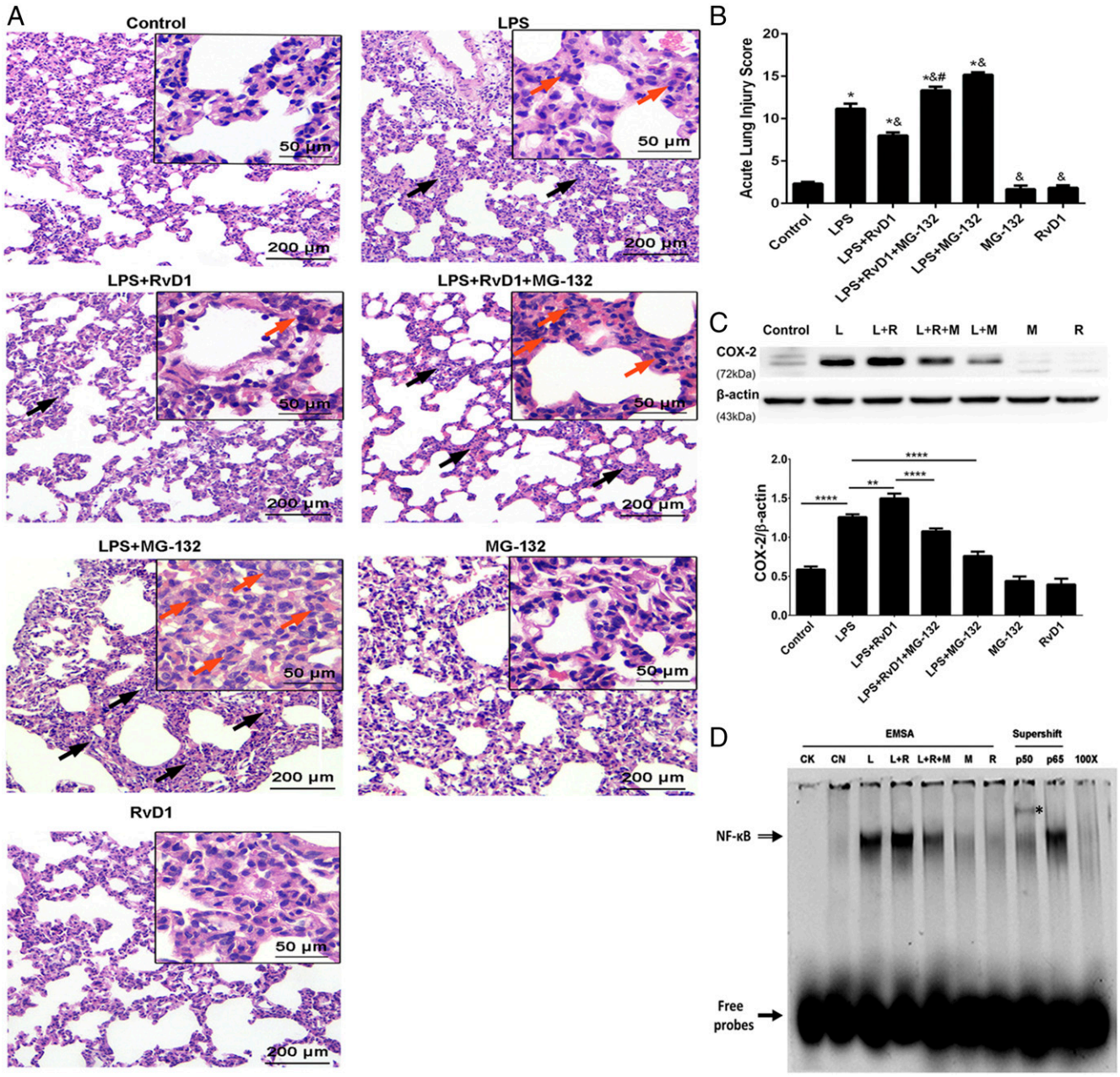

FIGURE 3. RvD1 facilitates the resolution of inflammation by promoting NF-κB p50–derived COX-2 expression in the ARDS model. Rats were i.v. injected with LPS (3 mg/kg) 12 h before they received tail vein injections with RvD1 (5 μg/kg) or an equivalent volume of ethanol. For treatment, rats were i.v. administered MG-132 at 1 h prior to RvD1 injection, whereas other groups received an equal volume of a DMSO saline solution. Rats were sacrificed 24 h after LPS exposure. Lung tissue samples were collected for morphological evaluation, Western blot, and EMSA supershift assays. (**A**) Representative photomicrographs of pulmonary histology, as shown by H&E staining. Original magnification, ×100 (inset, ×400). Black arrows indicate LPS-induced thickening of the alveolar walls and red arrows show neutrophil infiltration. (**B**) Acute lung injury score. (**C**) COX-2 protein expression was assessed via Western blot and analyzed by densitometry. Values were compared with β-actin expression. (**D**) NF-κB activation was determined via EMSA supershift assays with the nuclear protein extracts prepared from the lung tissues. EMSAs were used to quantify NF-κB activation in each group. Supershift assays were used to identify the activated NF-κB dimers in the LPS plus RvD1 group. EMSA supershift assays were performed as detailed in *Materials and Methods*. The NF-κB DNA–protein complexes (open arrow) were separated from the free probe (closed arrow) by electrophoresis in the EMSA. A supershift analysis was conducted with Abs directed against p50 and p65 to characterize specific NF-κB complexes in the LPS plus RvD1 group. Supershifted bands with an asterisk indicate binding of the p50 subunit. CK, negative control; CN, control group; L, LPS group; L+M, LPS plus MG-132 group; L+R, LPS plus RvD1 group; L+R+M, LPS plus RvD1 plus MG-132 group; M, MG-132 group; R, RvD1 group; 100×, competition group. Data are shown as mean ± SEM, $n = 5$–7 rats per treatment per group, and are representative of at least three independent experiments. $^{*}p < 0.05$ compared with the control group; $^{\&}p < 0.05$ compared with the LPS group; $^{\#}p < 0.05$ compared with the LPS plus RvD1 group. $^{**}p < 0.01$, $^{****}p < 0.0001$.

host. We used this self-limited model for our investigation. Recently, there has been growing recognition that RvD1 acts as an endogenous "braking signal" on excessive inflammation that tightly regulates the progression and timely resolution due to its potent anti-inflammatory and proresolving functions.

Prostanoids derived from COX-2 play fundamental roles in the multifarious bioactivity of COX-2. Several studies have demonstrated that PGE_2, the most abundant and prominent prostanoid in inflammation initiation, is involved in the processes leading to the classical signs of inflammation (36, 37). In contrast, PGD_2 par-

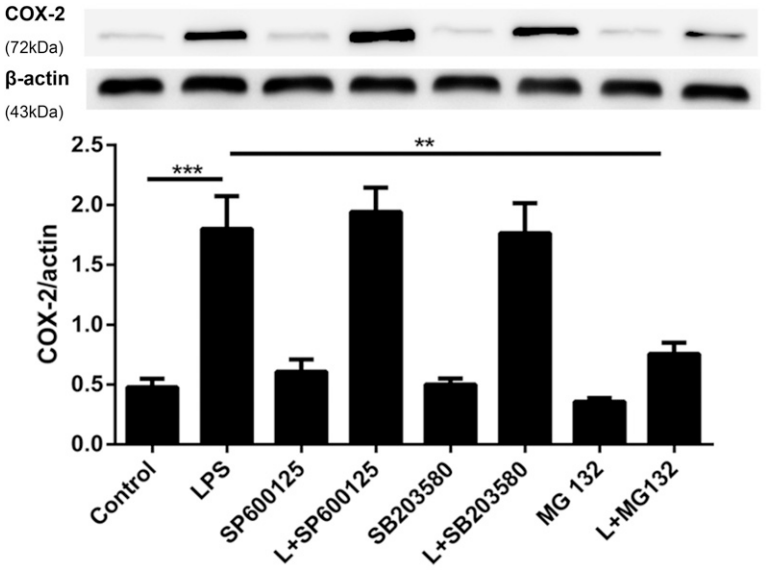

FIGURE 4. NF-κB is responsible for promoting the proresolving COX-2 protein expression in pulmonary fibroblasts. Primary pulmonary fibroblasts were incubated with 1 μg/ml LPS (L) for 24 h followed by administration of 100 nM RvD1 or vehicle (0.1% ethanol) for an additional 24 h, and 10 μM SP600125 (a JNK inhibitor), 10 μM SB203580 (a p38 MAPK inhibitor), and 10 μM MG-132 (an NF-κB inhibitor) were added 30 min prior to RvD1 administration. After incubation, the cells were harvested and sonicated. The expression of COX-2 was determined via Western blot. Cells were differentiated from lung tissues harvested from six rats per condition; $n = 8$ per treatment per group. Data are shown as mean ± SEM and are representative of at least four independent experiments. $^{**}p < 0.01$, $^{***}p < 0.001$.

ticipates in the control of resolution with its prolonged elevation during the later phase of inflammation (13, 38, 39). Consistent with these reports, our study clearly showed that, in both ex vitro and in vivo experiments, COX-2 was activated throughout the inflammatory response period. There was an initial COX-2 peak associated with maximal PGE_2 expression at the onset, and a secondary peak during the resolution phase that occurred concomitantly with increased PGD_2 synthesis. Moreover, PGE_2 and PGD_2, as well as the acetylation of COX-2 triggered by aspirin, actively mobilized the biosynthesis of other proresolving lipid mediators, such as lipoxins and resolvins, to dominate the resolution phase (14, 29, 40). Therefore, COX-2 may play a causative role in the switch from inflammation initiation to resolution (41).

Given the crucial role of COX-2 in the resolution of inflammation, as well as the potent proresolving capacity of RvD1, we investigated whether RvD1 could generate a positive loop in COX-2 activity-induced inflammatory resolution. Our previous work in pulmonary fibroblasts demonstrated the proinflammatory activity of COX-2, whereas the subsequent PGE_2 expression was abolished apparently by RvD1. These findings are in parallel with the large body of evidence demonstrating that RvD1 has potent anti-inflammatory activity via the suppression on COX-2 (32, 42,

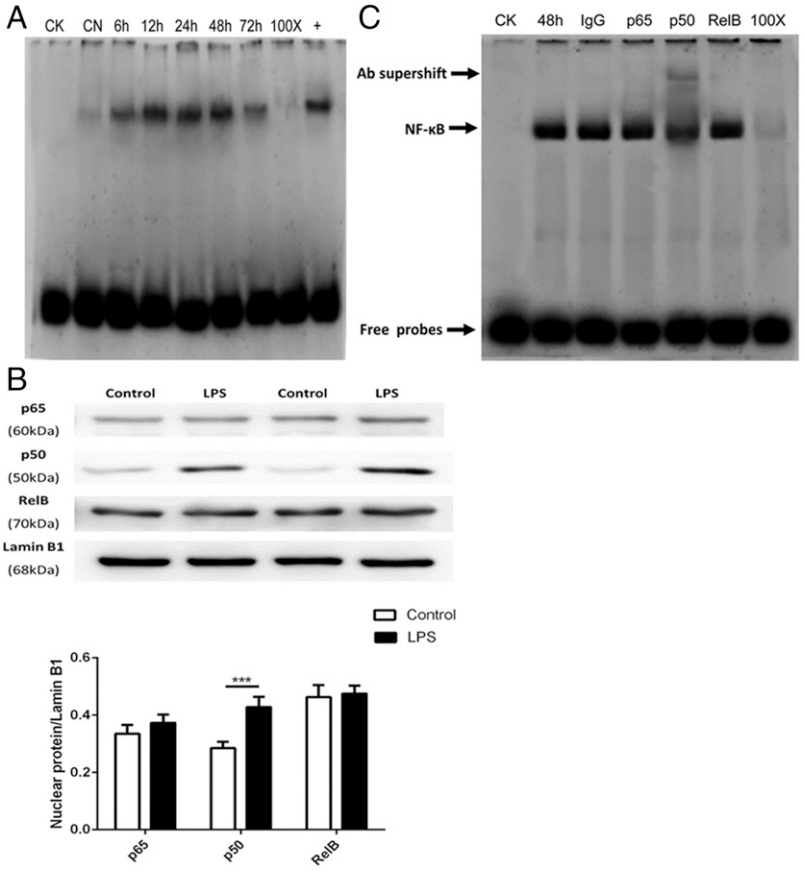

FIGURE 5. The formation of NF-κB p50/p50 homodimers in LPS-stimulated pulmonary fibroblasts occurs during resolution phase. Primary pulmonary fibroblasts were incubated with LPS (1 μg/ml) for 6, 12, 24, 48, and 72 h or with the equivalent volume of untreated medium for the control group. After incubation, the cells were harvested to isolate nuclear protein as detailed in *Materials and Methods*. (**A**) The time course of NF-κB activation was measured via EMSA. CK, negative control; CN, control group; 100×, competition group; +, positive group. (**B**) The nuclear translocation of p65, p50, and RelB was assessed via Western blot and analyzed via densitometry. Values were compared with lamin B1 expression. (**C**) Supershift assays were performed with NF-κB p50, p65, and RelB Abs to detect the DNA binding activity of nuclear protein extracts from primary pulmonary fibroblasts obtained 48 h after LPS stimulation. The specific NF-κB bands are indicated in the polyacrylamide gel with arrows, whereas only the Ab against p50 resulted in a significant supershift. CK, negative control; 48 h, cells stimulated with LPS for 48 h; IgG, preimmune IgG as Ab negative control; p50, p50 Ab group; p65, p65 Ab group; RelB, RelB Ab group; 100×, competition group. Cells were differentiated from lung tissues harvested from six rats per condition; $n = 6$ per treatment per group. Data in (A) and (C) are representative of three independent experiments. Data in (B) are shown as mean ± SEM and are representative of at least four independent experiments. $^{***}p < 0.001$.

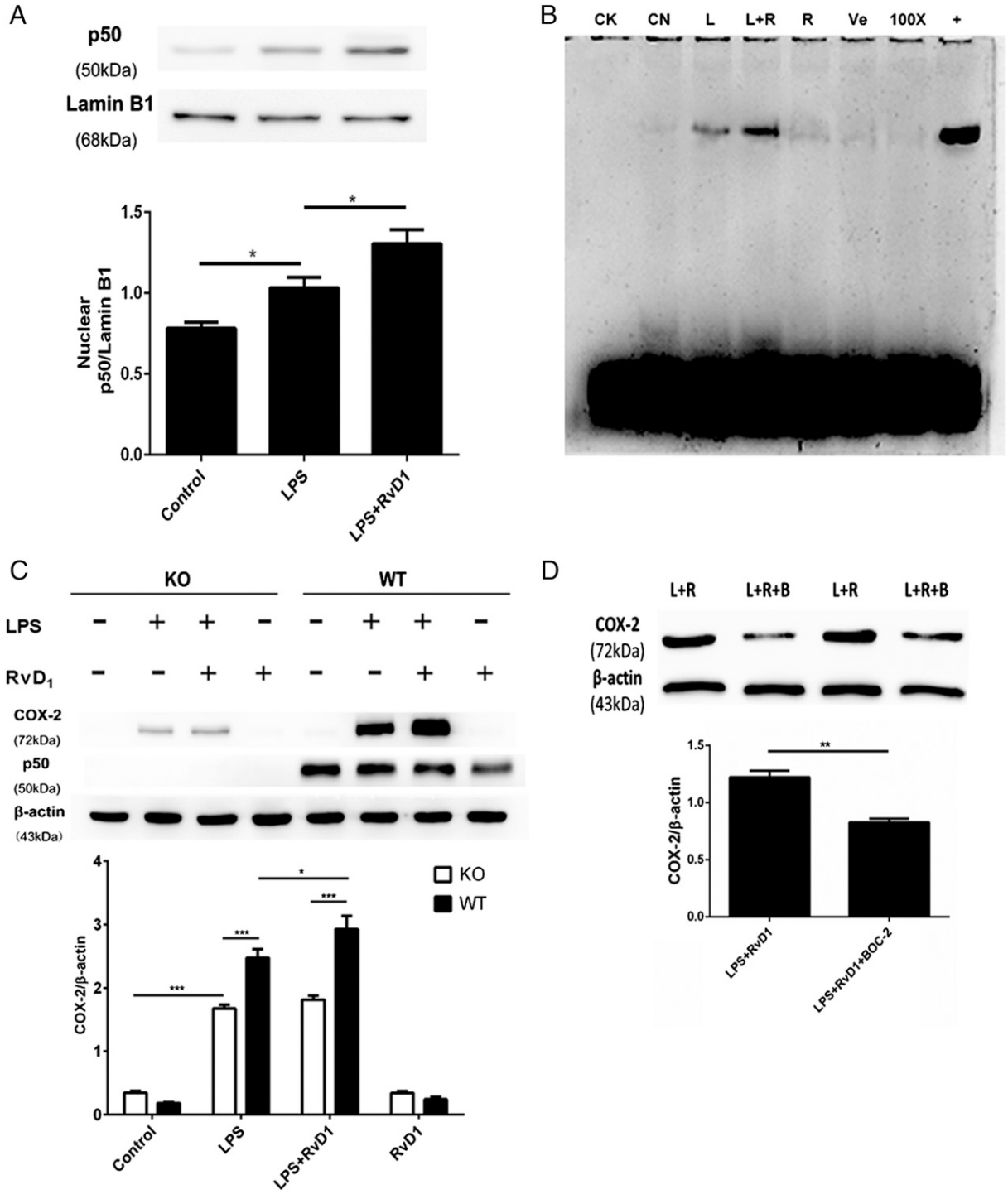

FIGURE 6. RvD1-mediated promotion of COX-2 expression in fibroblasts is mediated by NF-κB p50/p50 activation. (**A** and **B**) Primary pulmonary fibroblasts from rats were incubated with LPS (1 μg/ml) for 24 h, followed by the administration of 100 nM RvD1 or vehicle (0.1% ethanol) for an additional 24 h. After incubation, the cells were harvested to isolate nuclear proteins as detailed in *Materials and Methods*. (A) The expression of p50 in the nucleus was determined via Western blot and analyzed via densitometry. Values were compared with lamin B1 expression. (B) The activation of NF-κB was determined by EMSA assay. CK, negative control; CN, control group; L, LPS group; L+R, LPS plus RvD1 group; R, RvD1 group; Ve, vehicle group; 100×, competition group; +, positive group. (**C**) Primary pulmonary fibroblasts from NF-κB p50 KO (open bars) and WT mice (filled bars) were incubated with LPS (1 μg/ml) for 24 h followed by administration of 100 nM RvD1 or vehicle (0.1% ethanol) for an additional 24 h. After incubation, the cells were harvested and sonicated to obtain the whole protein. The expression of COX-2 and p50 was determined via Western blot. (**D**) Primary rat pulmonary fibroblasts were incubated with LPS (1 μg/ml) for 24 h, followed by the administration of 100 nM RvD1 for an additional 24 h; 10 μM BOC-2 was administered 30 min prior to the RvD1 treatment. After incubation, the cells were harvested and sonicated. COX-2 expression was assessed via Western blot. L+R, LPS plus RvD1 group; L+R+B, LPS plus RvD1 plus BOC-2 group. Cells in (A), (B), and (D) were differentiated from lung tissues harvested from six rats per condition. Pulmonary fibroblasts in (C) were differentiated from five mice per condition; $n = 5–6$ per treatment per group. Data are shown as mean ± SEM and are representative of at least three independent experiments. $^{*}p < 0.05$, $^{**}p < 0.01$, $^{***}p < 0.001$.

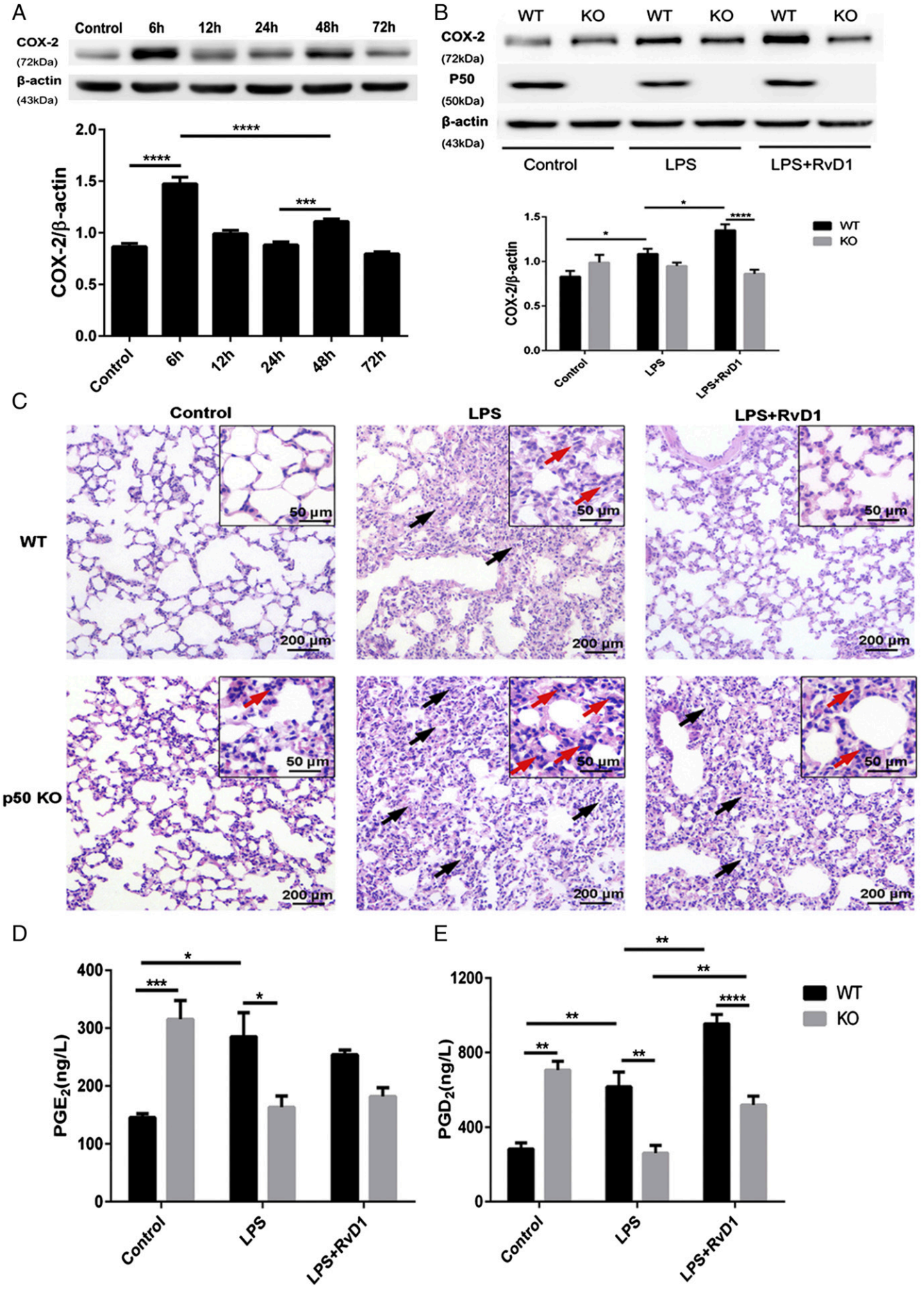
A
Control
6h
12h
24h
48h
72h
COX-2
(72kDa)
β-actin
(43kDa)
COX-2/β-actin
B
WT
KO
COX-2
(72kDa)
P50
(50kDa)
β-actin
(43kDa)
Control
LPS
LPS+RvD1
WT
KO
C
Control
LPS
LPS+RvD1
WT
p50 KO
50 μm
200 μm
D
PGE2(ng/L)
E
PGD2(ng/L)

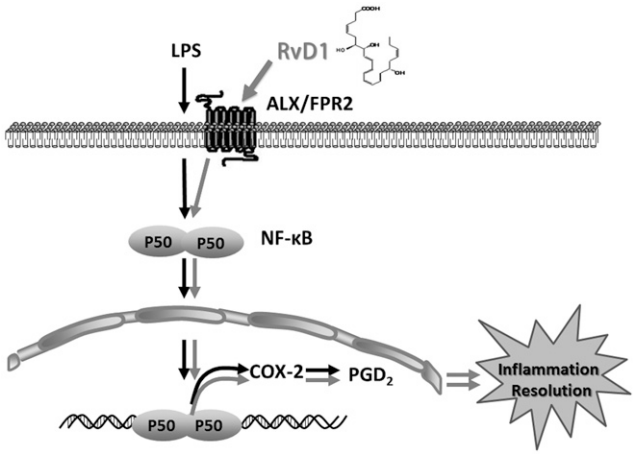

FIGURE 8. Proposed mechanisms underlying RvD1 that promote COX-2 expression and facilitate the resolution of inflammation.

43). Of interest, RvD1 also effectively increased the expression of COX-2 accompanied by elevated PGD_2 levels in the later phase of inflammation, suggesting a biphasic role of RvD1 in COX-2 expression during inflammation. In the present study, we further tested the effect of RvD1 on the biological activity of COX-2 in self-limited ARDS models established via LPS induction and demonstrated that RvD1 administration significantly upregulated COX-2 and PGD_2 expression during the later phase of inflammation, which accelerated resolution. Furthermore, lung injury scores were also reduced by RvD1 cotreatment, indicating that RvD1 may protect against lung injury via precipitating COX-2 expression and facilitating the resolution process.

Our present study indicates that only NF-κB was responsible for the COX-2 expression in the resolution stage, even though numerous signaling pathways are thought to regulate COX-2 (34, 44). Two NF-κB binding sites (p65/p50 and p50/p50) have been identified in the COX-2 gene region (44, 45), indicating that NF-κB p65/p50 and p50/p50 can serve as transcriptional regulators of COX-2 expression. Recently, studies have reported that RelB diminished cigarette smoke–induced COX-2 protein expression in lung fibroblasts, attenuating inflammation (46). The overexpression of RelB suppressed the inflammatory response and protected against lung injury (47). Therefore, we screened p65, p50, and RelB to clarify the role of NF-κB in the inflammation-resolving activity of COX-2. Surprisingly, our data from nuclear protein Western blot analysis and EMSA supershift assays showed that only the p50 homodimers were activated in the resolution phase. In agreement with our findings, several studies have identified p50/p50 as the predominant dimer during the later phase of inflammation (48–50). Of note, in rat carrageenan pleurisy, the proresolving activation of NF-κB has been found to be associated with increased COX-2 expression (50). The selective COX-2 inhibitor NS-398 has been reported to protract inflammatory response, whereas this treatment dose not decrease NF-κB DNA-binding activity during the resolving phase, which suggests that COX-2 may act downstream of NF-κB p50/p50 in the resolution of inflammation (50). Another study revealed that p50 homodimers predominantly resided in the NF-κB site and induced COX-2 transcriptional activation during the late phase of LPS-stimulated macrophage-associated inflammation (51). Thus far, NF-κB p50/p50 has been strongly implicated in COX-2 expression.

Next, we confirmed that RvD1 administration significantly promoted p50/p50 activation based on the accumulation of nuclear p50 protein and elevated DNA-binding activity, as shown by EMSA. Consistent with our findings, similar results have indicated that the addition of RvD1 to LPS-stimulated macrophages could activate p50/p50 to suppress TNF-α secretion, resulting in the restoration of efferocytosis (52). It is well appreciated that p50/p50 homodimers have a host-protective role. For instance, p50 homodimers suppressed the production of proinflammatory mediators (53) and upregulated anti-inflammatory cytokines, such as IL-10 (54). Moreover, they suppressed the classic macrophage proinflammatory response through inhibiting IFN-β and actively drove alternative macrophage (M2) polarization (55, 56), which is crucial for resolving inflammation (57). Moreover, the absence of p50 has been shown to aggravate pulmonary inflammation in *E. coli*–induced pneumonia (58) as well as result in more profound hepatic inflammation and severe fibrosis in chronic liver injury (59). Additionally, p50/p50 homodimers contribute to renal protection in ischemic preconditioning (60) and improve survival in kidney injury (49). Taken together, these findings indicate that the actions of p50/p50 activity may be a novel mechanism for the proresolving effect of RvD1 in regulating inflammation.

Two specific G protein–coupled receptors that bind RvD1 were recently identified as ALX/FPR2 and G protein–coupled receptor 32 (GPR32), and they are responsible to mediate the anti-inflammatory and proresolving bioactions of RvD1 (61). For example, RvD1 potently limits polymorphonuclear neutrophil infiltration and migration and enhances human macrophages phagocytosis upon binding to GPR32 and ALX/FPR2 (61–63). As GPR32 is a pseudogene in the rat and mouse (64), we administered an ALX/FPR2 antagonist (BOC-2) to determine whether the effect of RvD1 on COX-2 expression was mediated by ALX/FPR2. BOC-2 potently abrogated RvD1-induced upregulation of proresolving COX-2 production, indicating that the interaction between RvD1 and COX-2 depends on the ALX/FPR2 receptor.

To elucidate the essential role of NF-κB p50/p50 in the interaction between RvD1 and COX-2 in the resolution of ARDS, we used a proteasome inhibitor, MG-132, and p50-null mice. Pretreatment with MG-132 in a rat ARDS model abolished RvD1-induced upregulation of COX-2, which was correlated with severe pathological changes and elevated acute lung injury scores. Additionally, in the LPS and RvD1 cotreatment group, p50 KO mice showed impaired COX-2 induction and PG production; furthermore, they displayed excessive inflammatory cell infiltration in the

FIGURE 7. p50-deficient mice display impaired inflammation resolution and diminished COX-2 expression following RvD1 treatment. WT C57BL/6 mice were i.v. administered LPS (1 μg/ml) for 6, 12, 24, 48, and 72 h or the equivalent volume of sterile 0.9% saline as the control group. Lung tissue samples were collected after LPS administration for morphological evaluations, Western blot analyses, and ELISAs. (**A**) COX-2 protein expression was assessed via Western blot and analyzed via densitometry. Values were compared with β-actin expression. (**B**–**E**) Both WT and p50 KO mice were i.v. administered LPS (3 mg/kg) for 24 h, followed by the administration of RvD1 (5 μg/kg) or vehicle for an additional 24 h. After stimulation, right lungs were harvested. (B) The expression of COX-2 and p50 was determined via Western blot. (C) Representative photomicrographs of pulmonary histology, as shown by H&E staining. Original magnification, ×100 (inset, ×400). Black arrows indicate LPS-induced thickening of the alveolar walls and red arrows show neutrophil infiltration. (D and E) The concentrations of PGE_2 and PGD_2 in homogenized lung tissue were measured via ELISA. Data are shown as mean ± SEM, n = 5–6 mice per treatment per group, and are representative of at least three independent experiments. *$p < 0.05$, **$p < 0.01$, ***$p < 0.001$, ****$p < 0.0001$.

alveoli, which was strongly correlated with lung injury. In contrast, RvD1 significantly enhanced COX-2 and PGD_2 expression in WT mice, which is consistent with our previous results in fibroblasts. Notably, PGD_2 and PGE_2 were highly expressed in p50 KO mice even in the absence of a stimulus, and LPS had a dramatically decreased effect, indicating that other complementary host mechanisms are delicate and fragile for defense against stimulation. Collectively, we conclude that NF-κB p50/p50 is attributable, at least in part, to the proresolving effect of RvD1 on COX-2.

During ARDS, COX-2 inhibition caused by an NF-κB inhibitor and knockdown of the p50 gene led to prolonged inflammation and severe lung injury presented in our study, indicating critical roles for COX-2 in resolution of inflammation. Moreover, the concurrent addition of RvD1 and the NF-κB inhibitor or the treatment with RvD1 in the p50-null mice slightly relieved the lung injury or promoted PGD_2 production during the resolving phase, suggesting that the suppression of COX-2 expression induced by NF-κB inhibition did not absolutely block the protective bioactions of RvD1. The administration of RvD1 has been reported to bypass the adverse effect of a COX-2 inhibitor on myocardial infarction and afford cardioprotection (65). Moreover, as shown in the study by Schwab et al. (66) the resolution deficit induced by a COX-2 inhibitor was rescued with the exogenous administration of proresolving mediators such as resolvin E1 and protectin D1. All of these studies not only implied a pivotal function for COX-2 in homeostasis but also suggested that the COX-2 pathway is only one of the regulatory mechanisms of RvD1 involved in resolution. Additionally, other signaling pathways, such as the lipoxygenase pathway, may also induce the production of proresolving mediators to exert homeostatic function and promote timely resolution (66).

In several studies, RvD1 has been reported to inhibit COX-2 generation to protect tissues from inflammatory injury in many diseases, such as lung injury (32) and steatohepatitis (42). Unlike COX-2 genetic deletion or pharmacological inhibition by nonsteroidal anti-inflammatory drugs, both of which result in exacerbation of inflammatory injury and impairment of recovery, RvD1 upregulated proresolving COX-2 expression in the later phase of inflammation to prompt resolution. The biphasic role of RvD1 in regulating COX-2 expression allows modulation of COX-2 pathways at different stages of the inflammatory response and emphasized the homeostatic function of COX-2 in the host. Moreover, owing to the crucial role of COX-2 in the class switching of lipid mediators, RvD1 might regulate the production of other proresolving mediators in addition to PGD_2 to promote resolution.

Overall, our studies demonstrated that RvD1 can regulate NF-κB p50/p50 homodimer activation, dominate COX-2 expression, and subsequently monitor PGD_2 production to hasten resolution (Fig. 8). PGD_2 has been reported to exert diverse bioactions in promoting resolution; for example, PGD_2 exerts proresolving activity by targeting a neutrophil apoptosis mechanism (38). Moreover, it induces polymorphonuclear neutrophil 15-lipoxygenase activity, which is required for the subsequent generation of anti-inflammatory and proresolving lipid mediators, such as lipoxins, resolvins, and protectins (14, 67). Our findings confirm the biphasic activation of COX-2 in ARDS models of two different species and provide novel insights into the functions of NF-κB p50/p50 and COX-2 in the endogenous process of inflammation resolution, which enhances other natural resolution signaling pathways. Additionally, RvD1-induced promotion of COX-2 expression is beneficial for the complete resolution of inflammation, which partially occurs through the activation of ALX/FPR2 and NF-κB p50/p50 homodimers. This study provides evidence of the therapeutic potential of RvD1 in managing ARDS, emphasizing the importance of the endogenous natural resolving mechanism.

Acknowledgments

We thank Hong-Xia Mei and Xiang Xie for assisting with this study.

Disclosures

The authors have no financial conflicts of interest.

References

1. Rubenfeld, G. D., E. Caldwell, E. Peabody, J. Weaver, D. P. Martin, M. Neff, E. J. Stern, and L. D. Hudson. 2005. Incidence and outcomes of acute lung injury. *N. Engl. J. Med.* 353: 1685–1693.
2. Ranieri, V. M., G. D. Rubenfeld, B. T. Thompson, N. D. Ferguson, E. Caldwell, E. Fan, L. Camporota, and A. S. Slutsky, ARDS Definition Task Force. 2012. Acute respiratory distress syndrome: the Berlin definition. *JAMA* 307: 2526–2533.
3. Phua, J., J. R. Badia, N. K. Adhikari, J. O. Friedrich, R. A. Fowler, J. M. Singh, D. C. Scales, D. R. Stather, A. Li, A. Jones, et al. 2009. Has mortality from acute respiratory distress syndrome decreased over time?: a systematic review. *Am. J. Respir. Crit. Care Med.* 179: 220–227.
4. Matthay, M. A., L. B. Ware, and G. A. Zimmerman. 2012. The acute respiratory distress syndrome. *J. Clin. Invest.* 122: 2731–2740.
5. Serhan, C. N. 2017. Treating inflammation and infection in the 21st century: new hints from decoding resolution mediators and mechanisms. *FASEB J.* 31: 1273–1288.
6. Fullerton, J. N., and D. W. Gilroy. 2016. Resolution of inflammation: a new therapeutic frontier. *Nat. Rev. Drug Discov.* 15: 551–567.
7. Rajakariar, R., M. M. Yaqoob, and D. W. Gilroy. 2006. COX-2 in inflammation and resolution. *Mol. Interv.* 6: 199–207.
8. Basil, M. C., and B. D. Levy. 2016. Specialized pro-resolving mediators: endogenous regulators of infection and inflammation. *Nat. Rev. Immunol.* 16: 51–67.
9. Wallace, J. L. 2006. COX-2: a pivotal enzyme in mucosal protection and resolution of inflammation. *Sci. World J.* 6: 577–588.
10. Mochizuki, M., Y. Ishii, K. Itoh, T. Iizuka, Y. Morishima, T. Kimura, T. Kiwamoto, Y. Matsuno, A. E. Hegab, A. Nomura, et al. 2005. Role of 15-deoxy $\Delta^{12,14}$ prostaglandin J_2 and Nrf2 pathways in protection against acute lung injury. *Am. J. Respir. Crit. Care Med.* 171: 1260–1266.
11. Ulivi, V., R. Cancedda, and F. D. Cancedda. 2008. 15-deoxy-delta 12,14-prostaglandin J_2 inhibits the synthesis of the acute phase protein SIP24 in cartilage: involvement of COX-2 in resolution of inflammation. *J. Cell. Physiol.* 217: 433–441.
12. Colville-Nash, P. R., D. W. Gilroy, D. Willis, M. J. Paul-Clark, A. R. Moore, and D. A. Willoughby. 2005. Prostaglandin $F_{2\alpha}$ produced by inducible cyclooxygenase may contribute to the resolution of inflammation. *Inflammopharmacology* 12: 473–476.
13. Vong, L., J. G. Ferraz, R. Panaccione, P. L. Beck, and J. L. Wallace. 2010. A pro-resolution mediator, prostaglandin D_2, is specifically up-regulated in individuals in long-term remission from ulcerative colitis. *Proc. Natl. Acad. Sci. USA* 107: 12023–12027.
14. Levy, B. D., C. B. Clish, B. Schmidt, K. Gronert, and C. N. Serhan. 2001. Lipid mediator class switching during acute inflammation: signals in resolution. *Nat. Immunol.* 2: 612–619.
15. Fukunaga, K., P. Kohli, C. Bonnans, L. E. Fredenburgh, and B. D. Levy. 2005. Cyclooxygenase 2 plays a pivotal role in the resolution of acute lung injury. *J. Immunol.* 174: 5033–5039.
16. Quesnel, C., S. Marchand-Adam, A. Fabre, J. Marchal-Somme, I. Philip, S. Lasocki, V. Leçon, B. Crestani, and M. Dehoux. 2008. Regulation of hepatocyte growth factor secretion by fibroblasts in patients with acute lung injury. *Am. J. Physiol. Lung Cell. Mol. Physiol.* 294: L334–L343.
17. Flavell, S. J., T. Z. Hou, S. Lax, A. D. Filer, M. Salmon, and C. D. Buckley. 2008. Fibroblasts as novel therapeutic targets in chronic inflammation. *Br. J. Pharmacol.* 153(Suppl. 1): S241–S246.
18. Hsiao, H. M., R. E. Sapinoro, T. H. Thatcher, A. Croasdell, E. P. Levy, R. A. Fulton, K. C. Olsen, S. J. Pollock, C. N. Serhan, R. P. Phipps, and P. J. Sime. 2013. A novel anti-inflammatory and pro-resolving role for resolvin D1 in acute cigarette smoke-induced lung inflammation. *PLoS One* 8: e58258.
19. Lacy, S. H., C. F. Woeller, T. H. Thatcher, K. R. Maddipati, K. V. Honn, P. J. Sime, and R. P. Phipps. 2016. Human lung fibroblasts produce proresolving peroxisome proliferator-activated receptor-γ ligands in a cyclooxygenase-2-dependent manner. *Am. J. Physiol. Lung Cell. Mol. Physiol.* 311: L855–L867.
20. Wu, D., S. Zheng, W. Li, L. Yang, Y. Liu, X. Zheng, Y. Yang, L. Yang, Q. Wang, F. G. Smith, and S. Jin. 2013. Novel biphasic role of resolvin D1 on expression of cyclooxygenase-2 in lipopolysaccharide-stimulated lung fibroblasts is partly through PI3K/AKT and ERK2 pathways. *Mediators Inflamm.* 2013: 964012.
21. She, J., A. Goolaerts, J. Shen, J. Bi, L. Tong, L. Gao, Y. Song, and C. Bai. 2012. KGF-2 targets alveolar epithelia and capillary endothelia to reduce high altitude pulmonary oedema in rats. *J. Cell. Mol. Med.* 16: 3074–3084.
22. Shyamsundar, M., D. F. McAuley, R. J. Ingram, D. S. Gibson, D. O'Kane, S. T. McKeown, A. Edwards, C. Taggart, J. S. Elborn, C. S. Calfee, et al. 2014.

Keratinocyte growth factor promotes epithelial survival and resolution in a human model of lung injury. *Am. J. Respir. Crit. Care Med.* 189: 1520–1529.
23. Ware, L. B., and M. A. Matthay. 2002. Keratinocyte and hepatocyte growth factors in the lung: roles in lung development, inflammation, and repair. *Am. J. Physiol. Lung Cell. Mol. Physiol.* 282: L924–L940.
24. Bi, J., L. Tong, X. Zhu, D. Yang, C. Bai, Y. Song, and J. She. 2014. Keratinocyte growth factor-2 intratracheal instillation significantly attenuates ventilator-induced lung injury in rats. *J. Cell. Mol. Med.* 18: 1226–1235.
25. Tong, L., J. Bi, X. Zhu, G. Wang, J. Liu, L. Rong, Q. Wang, N. Xu, M. Zhong, D. Zhu, et al. 2014. Keratinocyte growth factor-2 is protective in lipopolysaccharide-induced acute lung injury in rats. *Respir. Physiol. Neurobiol.* 201: 7–14.
26. Hu, S., J. Li, X. Xu, A. Liu, H. He, J. Xu, Q. Chen, S. Liu, L. Liu, H. Qiu, and Y. Yang. 2016. The hepatocyte growth factor-expressing character is required for mesenchymal stem cells to protect the lung injured by lipopolysaccharide in vivo. *Stem Cell Res. Ther.* 7: 66.
27. Fang, X., L. Wang, L. Shi, C. Chen, Q. Wang, C. Bai, and X. Wang. 2014. Protective effects of keratinocyte growth factor-2 on ischemia–reperfusion–induced lung injury in rats. *Am. J. Respir. Cell Mol. Biol.* 50: 1156–1165.
28. Chen, S., X. Chen, X. Wu, S. Wei, W. Han, J. Lin, M. Kang, and L. Chen. 2017. Hepatocyte growth factor-modified mesenchymal stem cells improve ischemia/reperfusion-induced acute lung injury in rats. *Gene Ther.* 24: 3–11.
29. Serhan, C. N., S. Hong, K. Gronert, S. P. Colgan, P. R. Devchand, G. Mirick, and R. L. Moussignac. 2002. Resolvins: a family of bioactive products of omega-3 fatty acid transformation circuits initiated by aspirin treatment that counter proinflammation signals. *J. Exp. Med.* 196: 1025–1037.
30. Sun, Y. P., S. F. Oh, J. Uddin, R. Yang, K. Gotlinger, E. Campbell, S. P. Colgan, N. A. Petasis, and C. N. Serhan. 2007. Resolvin D1 and its aspirin-triggered 17R epimer. Stereochemical assignments, anti-inflammatory properties, and enzymatic inactivation. *J. Biol. Chem.* 282: 9323–9334.
31. Wang, Q., X. Zheng, Y. Cheng, Y. L. Zhang, H. X. Wen, Z. Tao, H. Li, Y. Hao, Y. Gao, L. M. Yang, et al. 2014. Resolvin D1 stimulates alveolar fluid clearance through alveolar epithelial sodium channel, Na,K-ATPase via ALX/cAMP/PI3K pathway in lipopolysaccharide-induced acute lung injury. *J. Immunol.* 192: 3765–3777.
32. Wang, B., X. Gong, J. Y. Wan, L. Zhang, Z. Zhang, H. Z. Li, and S. Min. 2011. Resolvin D1 protects mice from LPS-induced acute lung injury. *Pulm. Pharmacol. Ther.* 24: 434–441.
33. Wang, Q., Q. Q. Lian, R. Li, B. Y. Ying, Q. He, F. Chen, X. Zheng, Y. Yang, D. R. Wu, S. X. Zheng, et al. 2013. Lipoxin A_4 activates alveolar epithelial sodium channel, Na,K-ATPase, and increases alveolar fluid clearance. *Am. J. Respir. Cell Mol. Biol.* 48: 610–618.
34. Tsatsanis, C., A. Androulidaki, M. Venihaki, and A. N. Margioris. 2006. Signalling networks regulating cyclooxygenase-2. *Int. J. Biochem. Cell Biol.* 38: 1654–1661.
35. Ghosh, S., and M. S. Hayden. 2012. Celebrating 25 years of NF-κB research. *Immunol. Rev.* 246: 5–13.
36. Ricciotti, E., and G. A. FitzGerald. 2011. Prostaglandins and inflammation. *Arterioscler. Thromb. Vasc. Biol.* 31: 986–1000.
37. Funk, C. D. 2001. Prostaglandins and leukotrienes: advances in eicosanoid biology. *Science* 294: 1871–1875.
38. Rajakariar, R., M. Hilliard, T. Lawrence, S. Trivedi, P. Colville-Nash, G. Bellingan, D. Fitzgerald, M. M. Yaqoob, and D. W. Gilroy. 2007. Hematopoietic prostaglandin D_2 synthase controls the onset and resolution of acute inflammation through PGD_2 and 15-deoxyΔ^{12-14} PGJ_2. *Proc. Natl. Acad. Sci. USA* 104: 20979–20984.
39. Gilroy, D. W., P. R. Colville-Nash, D. Willis, J. Chivers, M. J. Paul-Clark, and D. A. Willoughby. 1999. Inducible cyclooxygenase may have anti-inflammatory properties. *Nat. Med.* 5: 698–701.
40. Clària, J., and C. N. Serhan. 1995. Aspirin triggers previously undescribed bioactive eicosanoids by human endothelial cell-leukocyte interactions. *Proc. Natl. Acad. Sci. USA* 92: 9475–9479.
41. Serhan, C. N., N. Chiang, and J. Dalli. 2015. The resolution code of acute inflammation: novel pro-resolving lipid mediators in resolution. *Semin. Immunol.* 27: 200–215.
42. Rius, B., E. Titos, E. Morán-Salvador, C. López-Vicario, V. García-Alonso, A. González-Périz, V. Arroyo, and J. Clària. 2014. Resolvin D1 primes the resolution process initiated by calorie restriction in obesity-induced steatohepatitis. *FASEB J.* 28: 836–848.
43. Gdula-Argasińska, J., J. Czepiel, J. Totoń-Żurańska, A. Jurczyszyn, P. Wołkow, T. Librowski, and W. Perucki. 2016. Resolvin D1 down-regulates CYP1A1 and PTGS2 gene in the HUVEC cells treated with benzo(a)pyrene. *Pharmacol. Rep.* 68: 939–944.
44. Kang, Y. J., U. R. Mbonye, C. J. DeLong, M. Wada, and W. L. Smith. 2007. Regulation of intracellular cyclooxygenase levels by gene transcription and protein degradation. *Prog. Lipid Res.* 46: 108–125.
45. Thomas, B., F. Berenbaum, L. Humbert, H. Bian, G. Béréziat, L. Crofford, and J. L. Olivier. 2000. Critical role of C/EBPδ and C/EBPβ factors in the stimulation of the cyclooxygenase-2 gene transcription by interleukin-1β in articular chondrocytes. *Eur. J. Biochem.* 267: 6798–6809.
46. Zago, M., A. Rico de Souza, E. Hecht, S. Rousseau, Q. Hamid, D. H. Eidelman, and C. J. Baglole. 2014. The NF-κB family member RelB regulates microRNA miR-146a to suppress cigarette smoke-induced COX-2 protein expression in lung fibroblasts. *Toxicol. Lett.* 226: 107–116.
47. McMillan, D. H., C. J. Baglole, T. H. Thatcher, S. Maggirwar, P. J. Sime, and R. P. Phipps. 2011. Lung-targeted overexpression of the NF-κB member RelB inhibits cigarette smoke-induced inflammation. *Am. J. Pathol.* 179: 125–133.
48. Mizgerd, J. P., M. L. Scott, M. R. Spieker, and C. M. Doerschuk. 2002. Functions of IκB proteins in inflammatory responses to *Escherichia coli* LPS in mouse lungs. *Am. J. Respir. Cell Mol. Biol.* 27: 575–582.
49. Panzer, U., O. M. Steinmetz, J. E. Turner, C. Meyer-Schwesinger, C. von Ruffer, T. N. Meyer, G. Zahner, C. Gómez-Guerrero, R. M. Schmid, U. Helmchen, et al. 2009. Resolution of renal inflammation: a new role for NF-κB1 (p50) in inflammatory kidney diseases. *Am. J. Physiol. Renal Physiol.* 297: F429–F439.
50. Lawrence, T., D. W. Gilroy, P. R. Colville-Nash, and D. A. Willoughby. 2001. Possible new role for NF-κB in the resolution of inflammation. *Nat. Med.* 7: 1291–1297.
51. Kang, Y. J., B. A. Wingerd, T. Arakawa, and W. L. Smith. 2006. Cyclooxygenase-2 gene transcription in a macrophage model of inflammation. *J. Immunol.* 177: 8111–8122.
52. Lee, H. N., J. K. Kundu, Y. N. Cha, and Y. J. Surh. 2013. Resolvin D1 stimulates efferocytosis through p50/p50-mediated suppression of tumor necrosis factor-α expression. *J. Cell Sci.* 126: 4037–4047.
53. Elsharkawy, A. M., F. Oakley, F. Lin, G. Packham, D. A. Mann, and J. Mann. 2010. The NF-κB p50:p50:HDAC-1 repressor complex orchestrates transcriptional inhibition of multiple pro-inflammatory genes. *J. Hepatol.* 53: 519–527.
54. Cao, S., X. Zhang, J. P. Edwards, and D. M. Mosser. 2006. NF-κB1 (p50) homodimers differentially regulate pro- and anti-inflammatory cytokines in macrophages. *J. Biol. Chem.* 281: 26041–26050.
55. Taetzsch, T., S. Levesque, C. McGraw, S. Brookins, R. Luqa, M. G. Bonini, R. P. Mason, U. Oh, and M. L. Block. 2015. Redox regulation of NF-κB p50 and M1 polarization in microglia. *Glia* 63: 423–440.
56. Porta, C., M. Rimoldi, G. Raes, L. Brys, P. Ghezzi, D. Di Liberto, F. Dieli, S. Ghisletti, G. Natoli, P. De Baetselier, et al. 2009. Tolerance and M2 (alternative) macrophage polarization are related processes orchestrated by p50 nuclear factor κB. *Proc. Natl. Acad. Sci. USA* 106: 14978–14983.
57. Martinez, F. O., A. Sica, A. Mantovani, and M. Locati. 2008. Macrophage activation and polarization. *Front. Biosci.* 13: 453–461.
58. Mizgerd, J. P., M. M. Lupa, M. S. Kogan, H. B. Warren, L. Kobzik, and G. P. Topulos. 2003. Nuclear factor-κB p50 limits inflammation and prevents lung injury during *Escherichia coli* pneumonia. *Am. J. Respir. Crit. Care Med.* 168: 810–817.
59. Oakley, F., J. Mann, S. Nailard, D. E. Smart, N. Mungalsingh, C. Constandinou, S. Ali, S. J. Wilson, H. Millward-Sadler, J. P. Iredale, and D. A. Mann. 2005. Nuclear factor-κB1 (p50) limits the inflammatory and fibrogenic responses to chronic injury. *Am. J. Pathol.* 166: 695–708.
60. Cao, C., S. Wang, L. Fan, X. Wan, X. Liu, and X. Chen. 2010. Renal protection by ischemic preconditioning is associated with p50/p50 homodimers. *Am. J. Nephrol.* 31: 1–8.
61. Krishnamoorthy, S., A. Recchiuti, N. Chiang, S. Yacoubian, C. H. Lee, R. Yang, N. A. Petasis, and C. N. Serhan. 2010. Resolvin D1 binds human phagocytes with evidence for proresolving receptors. *Proc. Natl. Acad. Sci. USA* 107: 1660–1665.
62. Norling, L. V., J. Dalli, R. J. Flower, C. N. Serhan, and M. Perretti. 2012. Resolvin D1 limits polymorphonuclear leukocyte recruitment to inflammatory loci: receptor-dependent actions. *Arterioscler. Thromb. Vasc. Biol.* 32: 1970–1978.
63. Krishnamoorthy, S., A. Recchiuti, N. Chiang, G. Fredman, and C. N. Serhan. 2012. Resolvin D1 receptor stereoselectivity and regulation of inflammation and proresolving microRNAs. *Am. J. Pathol.* 180: 2018–2027.
64. Haitina, T., R. Fredriksson, S. M. Foord, H. B. Schiöth, and D. E. Gloriam. 2009. The G protein-coupled receptor subset of the dog genome is more similar to that in humans than rodents. *BMC Genomics* 10: 24.
65. Gilbert, K., M. Malick, N. Madingou, C. Touchette, V. Bourque-Riel, L. Tomaro, and G. Rousseau. 2015. Metabolites derived from omega-3 polyunsaturated fatty acids are important for cardioprotection. *Eur. J. Pharmacol.* 769: 147–153.
66. Schwab, J. M., N. Chiang, M. Arita, and C. N. Serhan. 2007. Resolvin E1 and protectin D1 activate inflammation-resolution programmes. *Nature* 447: 869–874.
67. Serhan, C. N., and J. Savill. 2005. Resolution of inflammation: the beginning programs the end. *Nat. Immunol.* 6: 1191–1197.